

---

# Application of coherent anti-Stokes Raman scattering microscopy to image the changes in a paclitaxel-poly(styrene-*b*-isobutylene-*b*-styrene) matrix pre- and post-drug elution

---

Eunah Kang,<sup>1</sup> Haifeng Wang,<sup>1</sup> Il Keun Kwon,<sup>3</sup> Young-Ho Song,<sup>4</sup> Kalpana Kamath,<sup>4</sup> Kathleen M. Miller,<sup>4</sup> James Barry,<sup>4</sup> Ji-Xin Cheng,<sup>1</sup> Kinam Park<sup>1,2</sup>

<sup>1</sup>Weldon School of Biomedical Engineering, Purdue University, West Lafayette, Indiana 47907

<sup>2</sup>Department of Pharmaceutics, Purdue University, West Lafayette, Indiana 47907

<sup>3</sup>Department of Oral Biology and Institute of Oral Biology, School of Dentistry, Kyung Hee University, Seoul 130-701, South Korea

<sup>4</sup>Boston Scientific Corporation, Natick, Massachusetts 01760

Received 24 June 2007; revised 22 September 2007; accepted 16 October 2007

Published online 28 January 2008 in Wiley InterScience (www.interscience.wiley.com). DOI: 10.1002/jbm.a.31813

**Abstract:** Mapping the drug distribution in a polymeric film and following the subsequent changes that result during and after drug release is important to better understand the mechanism of drug release. This understanding leads to more efficiently designed tailor-made release profiles for drug-containing biomedical devices. Coherent anti-Stokes Raman scattering (CARS) microscopy was used for *in situ* imaging of local drug distribution in polymeric films, taking advantage of the three-dimensional (3D) resolution, high speed, high sensitivity, and noninvasiveness of the technology. Additionally, the morphological changes of poly(styrene-*b*-isobutylene-*b*-styrene) (SIBS) films during paclitaxel release were characterized by scanning electron microscopy, and drug release was quantitatively determined by high performance liquid chromatography. The time-dependent changes in the 3D distribution of paclitaxel in the polymer film

were visualized using CARS microscopy. CARS images showed that the paclitaxel was uniformly distributed throughout the SIBS matrix. Changes in the paclitaxel distribution during release were monitored using depth intensity profiles and showed that, upon exposure of the paclitaxel-loaded film to a release medium, the quantitative CARS intensity of paclitaxel decreased. These results indicate that paclitaxel was dissolved and depleted from the SIBS film during *in vitro* drug elution, supporting the use of CARS microscopy as an effective nondestructive technique for chemical imaging of paclitaxel elution dynamics in polymer films. © 2008 Wiley Periodicals, Inc. *J Biomed Mater Res* 87A: 913–920, 2008

**Key words:** drug-eluting stent; paclitaxel; poly(styrene-*b*-isobutylene-*b*-styrene) (SIBS); coherent anti-Stokes Raman scattering (CARS); microscopy

---

## INTRODUCTION

Drug-eluting stents (DESs) have been effectively used for controlling restenosis. Restenosis is a temporal vascular process, which has been associated with thrombosis, inflammation, migration of smooth muscle cell and proliferation, and endothelialization.<sup>1</sup> The success of DES mainly depends on the control of temporal vascular interplay, which can be modulated with the drug dose, spatial drug distribu-

tion, and the release rate, corresponding to vascular processes over time. The effective dose of an antiproliferative drug needs to be estimated for therapeutic effects due to toxicity to cells at high doses.<sup>2</sup> Spatial mapping of the locally released drug was made to study the drug partitioning in the vicinity of stent struts.<sup>3</sup> In addition, drug release from a DES should be sustained and controlled with consideration of pharmacological and temporal pathological procedures, depending on the mode of action of the drug. Various methods have been developed for controlling the local drug release from DESs.<sup>4–6</sup> Development of DES formulations with an appropriate dose and with the tailor-made release profile can be facilitated by understanding the three-dimensional (3D) drug distribution in the formulation and its time-dependent changes during release.

Correspondence to: K. Park; e-mail: kpark@purdue.edu  
Contract grant sponsor: National Institute of Health;  
contract grant number: HL078715  
Contract grant sponsor: Boston Scientific Corporation

The spatial information of paclitaxel in a polymer film that can be coated on the stent surface can be obtained with chemical imaging. Traditional chemical imaging tools include Fourier transform infra-red (FTIR),<sup>7-9</sup> confocal Raman microscopy,<sup>10,11</sup> nuclear magnetic resonance (NMR),<sup>12</sup> and secondary ion mass spectroscopy (SIMS),<sup>13,14</sup> all of which have limitations on resolution, sensitivity, or acquisition time of images. IR microscopy suffers from poor spatial resolution of 7  $\mu\text{m}$  due to its long excitation wavelength, and confocal Raman has low sensitivity not suitable for studying the drug distribution in polymer films. SIMS was used to trace chemical composition of the drug and polymer from stents,<sup>13</sup> but it is invasive to a sample and not able to provide 3D imaging *in situ*.

Coherent anti-Stokes Raman scattering (CARS) is a four-wave-mixing process in which a signal field at  $\omega_{\text{as}} = 2\omega_{\text{p}} - \omega_{\text{s}}$  is generated. The signal is enhanced when  $\omega_{\text{p}} - \omega_{\text{s}}$  is tuned to the vibrational frequency of a Raman band, thus providing a chemical selective contrast. As a nonlinear process, the signal is only generated at the laser focus, which provides inherent 3D resolution. In our previous study, the spatial distribution of paclitaxel in various polymer films was imaged using CARS microscopy with the resolution of 0.3 and 0.9  $\mu\text{m}$  in lateral axis and depth, respectively.<sup>15</sup> Recent developments including the use of epi-detection, picosecond pulse excitation, and laser-scanning have made CARS microscopy an attractive tool for molecular imaging.<sup>16,17</sup> In this study, CARS microscopy was used to examine the spatial distribution of paclitaxel and its release profiles from polymer films into isopropyl alcohol (IPA) solution.

## MATERIALS AND METHODS

### Materials

All the solvents and reagents used were purchased from Sigma-Aldrich (Berkeley, CA) and used as received. Paclitaxel (FW 854) and poly(styrene-*b*-isobutylene-*b*-styrene) (SIBS) were kindly supplied by Boston Scientific (Natick, MA). The specific polymer studied in these experiments has polydispersity index of 1.36 with a  $M_n$  of 109,000 and is representative of that used in commercial DES product. SIBS was studied extensively as the base materials for developing Taxus<sup>TM</sup> DES (Boston Scientific, Natick, MA).<sup>18-20</sup> The coating formulation containing 35 wt % paclitaxel and 65 wt % SIBS in a mixture of tetrahydrofuran and toluene (5:95 by weight) was used to coat films onto clean cover glass (15  $\times$  15 mm<sup>2</sup>). The thickness of the coated films was  $\sim$ 30  $\mu\text{m}$ , as measured by a confocal laser-scanning microscope.

### Paclitaxel release study

Paclitaxel release from SIBS films was carried out using isopropyl alcohol (100 vol % IPA) or 30 vol % IPA in phos-

phate-buffered saline (PBS) as release media. IPA in PBS is an accepted medium for accelerated drug release testing of Taxus product. As an "accelerated" medium, it is nonphysiological and has been shown to be applicable to SIBS-based matrix delivery system. Paclitaxel was released from a SIBS film during immersion of the film in 10 mL of either release medium at room temperature under static conditions. After removal at predetermined times of 1 mL of release medium for paclitaxel analysis, the remaining total release medium was replaced at each sampling interval. Acetonitrile (0.5 mL) was added to each sample and the paclitaxel concentration was analyzed using a high-performance liquid chromatography (HPLC) (Agilent 1100 series, Agilent Technologies, Wilmington, DE). A symmetry column (C18, Waters, Milford, MA) and a diode array detector at 227 nm were used for paclitaxel detection. Samples were run at the flow rate of 1.0 mL/min at 37°C. The mobile phase was a 50:50 mixture of acetonitrile and water.

### Scanning electron microscopic observation

The SIBS films were cut into  $\sim$ 0.5 cm-by-0.5 cm sections while immersed in liquid nitrogen and then attached on a Si wafer with double side tape. The wafer was then placed upright in a slit holder and secured with cryo adhesive. Samples were first plunged into a liquid nitrogen slush to freeze, transferred to the preparation stage of an Alto 2500 cryo-system (Gatan, Warrendale, PA) and coated with platinum prior to transfer into a scanning specimen chamber. The cross-sectional and surface images were obtained with a NOVA nano field emission scanning electron microscopy (FE-SEM) (FEI Company, Hillsboro, OR) with an Everhart-Thornley secondary electron detector and a through-the-lens detector, operating primarily at 2-3 kV, aperture 6, spot size 3 and 4.5-5 mm working distance.

### CARS microscopy

Details of our CARS microscope were described in our previous publication.<sup>15</sup> Briefly, two Ti:sapphire lasers (Mira900, Coherent, Santa Clara, CA) were tightly synchronized with an average timing jitter of 100 fs to generate 2.5 ps pump and Stokes beams at frequency  $\omega_{\text{p}}$  and  $\omega_{\text{s}}$ , respectively ( $\omega_{\text{p}} > \omega_{\text{s}}$ ). The two excitation beams were collinearly combined and were directed into a confocal laser-scanning microscope (FV300/IX70, Olympus America, Melville, NY).<sup>21,22</sup> The CARS signal was detected in the forward direction with a photomultiplier tube.

To study the change in paclitaxel distribution within the polymer during *in vitro* drug release, a glass slide coated with a paclitaxel-loaded SIBS film was attached to the bottom of a glass-petri dish (MatTek, Ashland, MA). A 1 cm diameter area of the polymer film was exposed to the release medium by adding the release medium. The release medium of 2 mL was added and replaced with fresh medium at predetermined times. CARS images were captured over time through the film depth of Z axis to examine the change of paclitaxel distribution in the film during release.

## RESULTS

Paclitaxel release from SIBS films was characterized by measuring the amount of paclitaxel released into medium as a function of time, as well as by examining the resulting film morphology. SIBS films loaded with 35% paclitaxel were exposed to either 100% IPA or 30% IPA in phosphate-buffered solution (PBS). The measured solubility of paclitaxel in 100% IPA and 30% IPA was  $>10$  mg and  $0.105 \pm 0.026$  mg/mL, respectively. The two release media were used to study the paclitaxel release mechanism from SIBS films. Paclitaxel release profiles are shown in Figure 1(A). In 100% IPA,  $\sim 85\%$  of paclitaxel was released within 2 h while only 50% of paclitaxel was released after 13 days in 30% IPA. The SIBS films loaded with the same amount of paclitaxel resulted in different release profiles depending on the release medium used. The observation that all paclitaxel was released in a matter of hours into 100% IPA indicates that IPA could diffuse into the SIBS film to accelerate the paclitaxel dissolution and subsequent release.

The experimental data were fitted to two mathematical models, the Higuchi model and the power law.<sup>23,24</sup> The curve fit to each model of the paclitaxel release profile is presented in Figure 1(B,C). The Higuchi model assumes pseudo-steady state approach, which is based on the condition that initial drug concentration ( $C_0$ ) in the polymer matrix (i.e., SIBS film) is much higher than the solubility ( $C_s$ ) of the drug in the polymer matrix. Thus, dissolved drugs and dispersed drugs (i.e., undissolved solid drugs) coexist in the polymer matrix. The presence of well dispersed paclitaxel in nano/microparticles in SIBS films meets the criteria of suspended, i.e., dispersed, drug. As the dissolved paclitaxel is released from the surface of the film, the dispersed paclitaxel particles are then dissolved to maintain the saturation concentration ( $C_s$ ), and thus, a constant concentration gradient. After the surface has released all the available drug, and the underlying dispersed drug has dissolved, the dissolved drug boundary begins to be released into the environment.

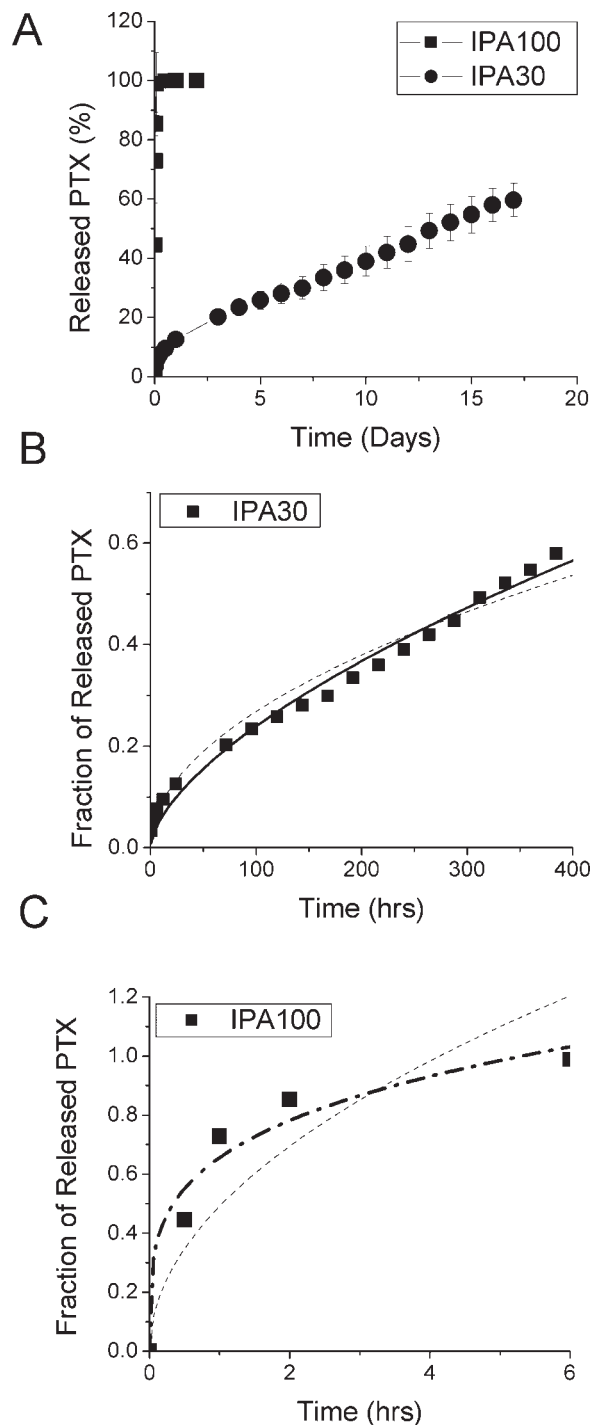
In the Higuchi model, the cumulative amount of drug released ( $M$ ) is described by the following equation:

$$M_t = S[DC_s(C_0 - C_s)t]^{1/2} = k't^{1/2}$$

where  $S$  is the surface area and  $D$  is the diffusion coefficient of paclitaxel through the SIBS matrix. All parameters in the Higuchi equation are constants and so the equation can be simplified to yield a straight line as a function of  $t^{1/2}$ . The paclitaxel release data were also fit to the power law:

$$\frac{M_t}{M_\infty} = kt^n$$

**Figure 1.** Paclitaxel release as a function of time in 100% IPA (IPA100) and 30% IPA (IPA30) (A), and model fitting for the release data in IPA30 (B) and IPA100 (C). Solid line and dashed line indicate Power model and Higuchi equation, respectively.



where  $M_t$  and  $M_\infty$  are cumulative amount of drug released at time  $t$  and infinite time at the constant

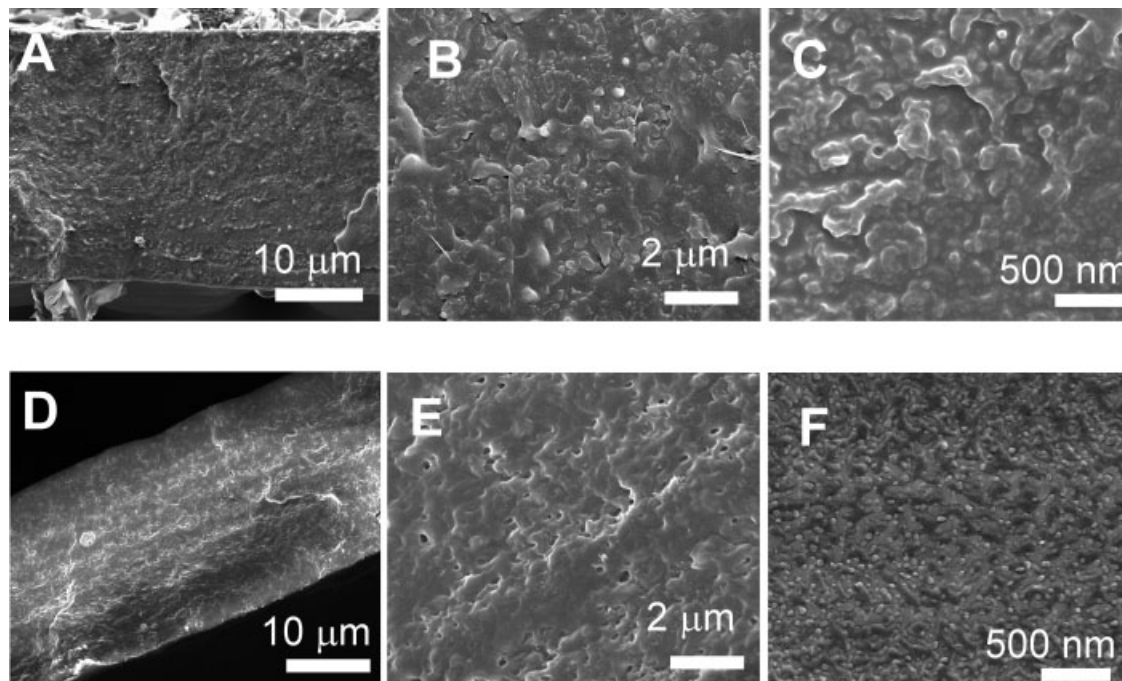


**Figure 2.** SEM images of the cross section and surface of the films before paclitaxel release at  $t = 0$  (A, B, and C) and after paclitaxel release at  $t = 1$  day (D, E, and F). Panels A and D are images of the cross sections of the film. Panels B and E are magnified images of panels A and D, respectively. Panels C and F are the images of the film surface. Paclitaxel was completely released in IPA100 for 2 h.

loading dose, respectively. A constant of  $k$  is related to structural and geometrical characteristics, and  $n$  is the release exponent, indicative of the mechanism of drug release.

The values of  $k'$  for the Higuchi model were 0.49 and 0.03 for 100% IPA and 30% IPA, respectively. The Higuchi model was not able to fit the experimental data very well for paclitaxel release in 100% IPA. The power law model could fit the experimental data better, but the low calculated  $n$  value of 0.25 indicated that there were not enough data points to have a meaningful statistical fitting of the data. This was most likely due to the extremely fast release of paclitaxel from SIBS films incubated in 100% IPA. All paclitaxel was released in about 6 h [Fig. 1(C)], and an insufficient number of data points were able to be obtained. For paclitaxel release into 30% IPA, both Higuchi and power law models were able to fit the data very well [Fig. 1(B)]. The  $n$  value was 0.62, indicating that the paclitaxel release was controlled by both diffusion of paclitaxel through the SIBS film and polymer chains undergoing relaxation by the imbibed solvent.<sup>25</sup> The Higuchi equation is the special case of the power law where  $n = 0.5$ , and the fact that the calculated  $n$  value of 0.62 suggests that the dominating paclitaxel release mechanism is the diffusion of dissolved paclitaxel through the SIBS matrix.

Morphology of paclitaxel-loaded SIBS films was examined by FE-SEM. FE-SEM images were taken of

the films before and after drug release in 100% IPA. All the paclitaxel was extracted after 2 h of incubation in 100% IPA. At  $t = 0$ , images of the cross section of the SIBS film showed that there were a large number of micro/nanospherical particulates dispersed throughout the film [Fig. 2(A)]. Those particulates were even more visible at higher magnification of both cross section [Fig. 2(B)] and film surface [Fig. 2(C)]. At  $t = 1$  day, when most of the loaded paclitaxel was released, the SEM images showed the presence of isolated void areas [Fig. 2(D)]. The void areas became more apparent at higher magnification of cross section [Fig. 2(E)] and film surface [Fig. 2(F)]. Numerous pebble-like structures on the surface of the film were observed, which is a similar feature observed by others.<sup>18</sup> Those structures became visible after 35% paclitaxel was released to expose void spaces.

The spatial distributions, especially the depth profiles, of paclitaxel in the SIBS films were examined by CARS microscopy. To provide chemical identities of paclitaxel and SIBS, chemical-specific Raman shifts were identified from Raman spectra [Fig. 3(A)]. The phenyl groups and alkyl bonds of paclitaxel contribute to a strong aromatic CH stretch vibration band centered at  $3070\text{ cm}^{-1}$  and to  $\text{CH}_3$  stretch vibration at  $2939\text{ cm}^{-1}$ , respectively. The Raman spectrum of SIBS also showed peaks at  $3052\text{ cm}^{-1}$  for aromatic CH stretch vibration of the styrene monomer and at  $2910\text{ cm}^{-1}$  for asymmetric

CH<sub>2</sub> stretching. Thus, the CH stretching region was not able to provide the peaks unique to paclitaxel. As an alternative, the fingerprint region was examined. Paclitaxel has peaks at 1723 cm<sup>-1</sup> for C=O bond and 1603 cm<sup>-1</sup> for C=C bond, whereas SIBS has characteristic peak only at 1603 cm<sup>-1</sup>. Thus, the peak at 1723 cm<sup>-1</sup> for C=O stretching was used for paclitaxel imaging.

Both nonresonant and resonant fields contribute to CARS signals, inferring that the two fields shift the shape of CARS spectra, generating the peak and the dip positions for each Raman band. Thus, accurate Raman shifts were resolved by taking CARS spectra, which were recorded by tuning the Stokes laser frequency by point by point. The CARS signal from paclitaxel or SIBS films was normalized by the nonresonant signal from the glass. The CARS spectra at 3000 and 1600 cm<sup>-1</sup> region are shown in Figure 3(B,C), respectively. A strong peak and a dip of paclitaxel were observed at 3060 and 3090 cm<sup>-1</sup>, respectively, from aromatic CH stretching as correspondence to Raman spectra. SIBS, however, also has a peak at this Raman shift because it has the aromatic CH bond on the benzyl group of the side chain, which is the chemically equivalent bond of paclitaxel. The peak at 3060 cm<sup>-1</sup> did not differentiate the Raman band between paclitaxel and SIBS [Fig. 3(B)]. To distinguish chemical-specific Raman band of paclitaxel, CARS spectra in the finger print region were taken for SIBS and paclitaxel [Fig. 3(C)]. The peak and the dip characteristic of paclitaxel were observed at 1700 and 1730 cm<sup>-1</sup>, while spectrum of SIBS at this region was dominated by the nonresonant background. The subtraction between the peak and dip only presents chemical-specific intensity of paclitaxel and cancels SIBS signal. The difference signal between the peak at 1700 cm<sup>-1</sup> and the dip 1730 cm<sup>-1</sup> of paclitaxel, and the peak of SIBS at 2840 cm<sup>-1</sup> were determined to image paclitaxel molecules and SIBS matrix in paclitaxel-loaded SIBS films.

CARS spectra for pure paclitaxel and paclitaxel dispersed in SIBS films may have different peak positions because the intensity of the nonresonant signal can be altered depending on the molecular concentration of paclitaxel and molecular environment of the polymer matrix. The strong peak at 1600 cm<sup>-1</sup> for C=C bond of paclitaxel may influence the peak position of C=O bond, depending on the concentration of paclitaxel. Thus, CARS spectra in the fingerprint region were recorded again using 35% paclitaxel/SIBS film as shown in Figure 3(D). The appearance of the peak shift at 1710 cm<sup>-1</sup> was ideal for the 35% paclitaxel/SIBS films, and the peak at 1710 cm<sup>-1</sup> and the dip at 1730 cm<sup>-1</sup> were used for imaging.

SIBS films loaded with 35% paclitaxel were imaged at each Raman shift of 1710, 1730, and 2840 cm<sup>-1</sup>. CARS images showed that paclitaxel embedded in SIBS films was homogeneous throughout the film depth. Paclitaxel was uniformly distributed without any large aggregates (Panels A–C in Fig. 4). For quantitative analysis of the paclitaxel concentration, depth profiles of CARS intensity through the polymer film were used for mapping drug distribution and monitoring drug release. Figure 4(D) presents depth profiles of CARS intensity through the SIBS film at each Raman shift. For the chemical-specific signal of the paclitaxel molecule, resonant molecular vibration from CARS was isolated from the nonresonant background. To remove nonresonant background, the depth intensity profile taken at 1730 cm<sup>-1</sup> was subtracted from the profile taken at 1710 cm<sup>-1</sup>. The difference intensity between the two wavelengths was then normalized by the intensity at 1730 cm<sup>-1</sup>, presenting the chemical-specific vibration of paclitaxel [Fig. 4(E)]. Normalized difference CARS intensity is proportional to the number of molecules, i.e., the paclitaxel concentration.

Paclitaxel release over time was monitored by evaluating changes of the depth intensity profile. Paclitaxel-loaded SIBS films were exposed to 100% IPA and 30% IPA in PBS, and changes of the depth profile were examined (Fig. 5). The resonant CARS contrast from paclitaxel showed uniform intensity though the depth of the polymer film before drug release, i.e., at  $t = 0$ . On exposure to 100% IPA, the intensity of CARS depth profiles was significantly reduced after only 8 min. This result showed that paclitaxel was depleted from the SIBS matrix as IPA was imbibed into the SIBS film. The data on depth profiles showed that the gradient decreased near the film surface, indicating that all the paclitaxel near the surface was completely depleted. As the drug elution time increased, the gradient became steeper, partly supporting the Higuchi model where the drug-depleted region migrated from the surface toward the inner, bulk of the film. After a drug elution time of 64 min, CARS intensity was close to zero and the profile became flat. According to the HPLC analysis, 72% of paclitaxel was released by this time. The paclitaxel depth profiles of SIBS films incubated in the 30% IPA are shown in Figure 5(B). The depth profiles of the paclitaxel resonant signal constructed over time showed that paclitaxel was released at a considerably slower rate in this medium, as shown in the HPLC analysis [Fig. 1(A)]. The gradient changes of depth profile were moderate compared to that released in pure IPA due to the slower release. The intensity of depth profiles was lower near the surface of polymer matrix, again indicating that paclitaxel was released from the surface.

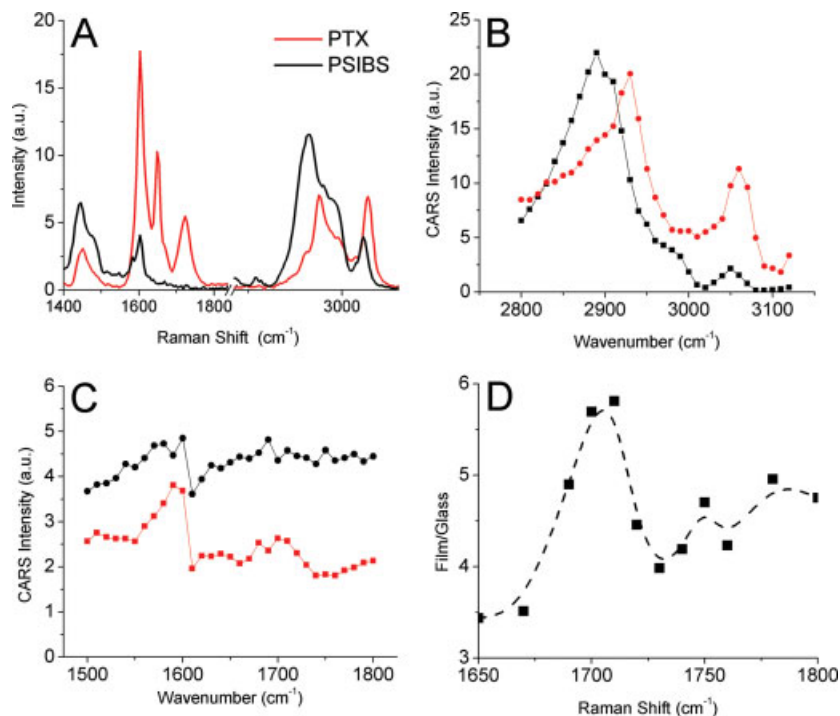


**Figure 3.** Raman and CARS spectra of paclitaxel and SIBS. Raman spectra of paclitaxel and SIBS (A), CARS spectra of paclitaxel and PSIBS at  $3060\text{ cm}^{-1}$  (B), CARS spectra of paclitaxel and SIBS at  $1600\text{ cm}^{-1}$  region (C), and CARS spectra at the  $1700\text{ cm}^{-1}$  region for 35% paclitaxel/SIBS film (D). [Color figure can be viewed in the online issue, which is available at [www.interscience.wiley.com](http://www.interscience.wiley.com).]

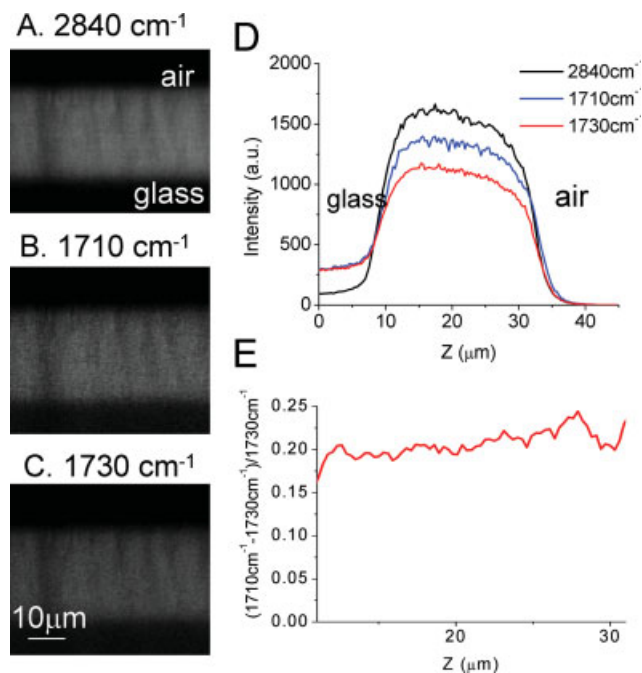


**Figure 4.** CARS depth images and depth profiles of the SIBS film loaded with 35% paclitaxel before drug release. CARS depth images taken at  $2840\text{ cm}^{-1}$  (A),  $1710\text{ cm}^{-1}$  (B), and  $1730\text{ cm}^{-1}$  (C). (D) Depth profiles of the images taken at three wave numbers. (E) Difference intensity profile between  $1710\text{ cm}^{-1}$  and  $1730\text{ cm}^{-1}$ , normalized by the intensity at  $1730\text{ cm}^{-1}$ . [Color figure can be viewed in the online issue, which is available at [www.interscience.wiley.com](http://www.interscience.wiley.com).]

The change of film morphology was examined using XY images of the films taken at different depth by CARS microscopy before and after paclitaxel release. Different depths of the same spot of the same sample were taken during paclitaxel release in 100% IPA. Before paclitaxel release ( $t = 0$ ), the film from XY images was uniform in both bottom and top (the first column in Fig. 6). After paclitaxel release for 60 min, XY images showed the waved feature of the film, indicating that depletion of paclitaxel generates the roughness of the film in both mid-depth and surface (the second column in Fig. 6).

## DISCUSSION

Numerous drug delivery systems have been developed for controlling drug release kinetics. However, only a small number of studies have visualized the spatial distribution of the loaded drug molecules, especially without labeling the drugs. Understanding the spatial drug distribution and its time-dependent changes during drug release can lead to elucidation of drug release mechanisms, and better prediction of *in vivo* drug release profiles. In this study, CARS microscopy was used to image the spatial distribution of paclitaxel in SIBS films and to follow the time-dependent changes during the release experiments.

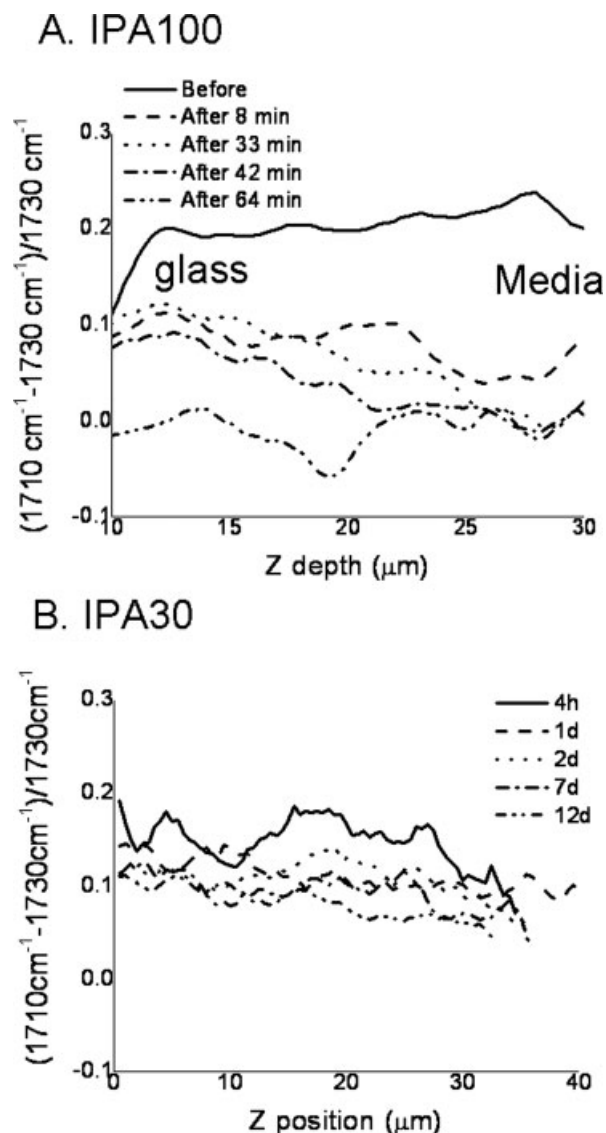


**Figure 5.** Depth profiles of paclitaxel in the SIBS film as a function of the release time in 100% IPA (A) and 30% IPA (B).

CARS depth profiles of paclitaxel during release from the SIBS matrix in IPA solution showed that it was feasible to image the spatial distribution of the loaded drug and its redistribution over the course of the release experiment. In addition, morphological changes of the drug-loaded polymer matrix were observed during drug release due to absorption of medium into the film. CARS microscopy was effective in analyzing the dynamic process of drug release and monitoring the changes in the spatial distribution of paclitaxel in the polymer films. IPA was used to accelerate the release of paclitaxel so that the dynamic release of paclitaxel from the SIBS films could be studied using CARS in a reasonably short time period. Paclitaxel in the SIBS matrix was

imaged in the finger print region under an aqueous environment. Imaging in the finger print region is useful for a drug and polymer combination; both of which have the same chemical identity at the CH stretching region, such as that shown for paclitaxel and SIBS. Furthermore, imaging in the finger print region provides the advantage of avoiding the overlap of the water peak around  $3200\text{ cm}^{-1}$  with the target peaks, in the event that the drug release study is done in an aqueous medium. A single drug particle was followed to monitor local drug dissolution and release over the course of time.<sup>15</sup> Under conditions where the drug aggregates are not discernible due to uniform distribution of the drug at the molecular and submicron level in the polymer matrix, depth intensity profiles can be employed to compare the relative drug concentrations. The trend in the depth profiles provides a qualitative spatial drug release pattern. Depth profiles of paclitaxel release using CARS microscopy provided new information, collected noninvasively, about the spatial distribution and temporal release of even an unlabeled drug.

Observing the changes in the morphology of a drug-loaded film before and after drug release can also lead to developing a sustainable mechanism for drug release. Atomic force microscopy (AFM), frequently used for *in situ* observation of drug release from film surfaces, can only provide information relative to the surface and is not able to image bulk dissolution of the drug. It is also technically difficult, since the drug may saturate and crystallize in the small scanning chamber.<sup>18</sup> Access to the open chamber placed in a sample stage of a CARS microscopy system offers simple maintenance of the sink condition by allowing easy replacement of the release medium. CARS also allows *in situ* imaging of the film in mid-depth, in addition to the surface, and in a noninvasive way without interruption of the release experiment. These unique properties of CARS were essential in studying the drug release mechanisms from the paclitaxel-SIBS films.

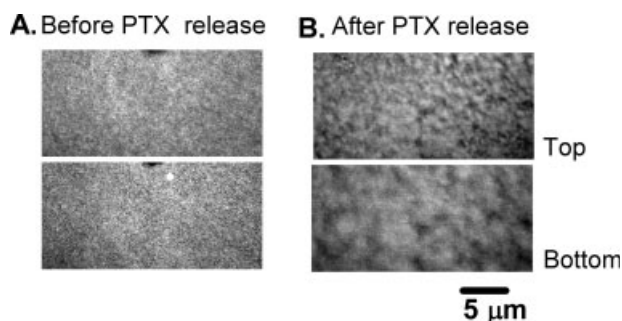


**Figure 6.** CARS images of the XY plane in the bottom and top of the film at  $t = 0$  (A) and  $t = 60$  min (B) of paclitaxel release in 100% IPA. The top and bottom images of the SIBS film are shown. The images were taken at  $2840\text{ cm}^{-1}$ .

Many controlled release systems have been studied using mathematical models to elucidate drug release mechanisms.<sup>24,26</sup> Models are developed based on certain assumptions, and thus whether each model can describe experimental data well or not depends on the experimental conditions. In this study, the Higuchi equation was a close fit to our system wherein the paclitaxel was released in a 30% IPA solution. The data on paclitaxel released into 100% IPA, however, did not fit well to either the Higuchi equation or the power law model. This is most likely attributed to the extremely fast release of the loaded paclitaxel due to the IPA imbibed into the polymer film. The study of CARS depth profiles provided direct observation of spatial and temporal drug distribution and closely matched the drug release kinetics. Combining the depth profiles with the mathematical modeling can provide a wealth of information to establish or validate mechanisms of drug release.

While CARS has been very useful in the study of drug release from polymer films without labeling the drug, it is important to know the limitation of the technique in terms of sensitivity. The difference CARS signal of paclitaxel was sensitive to low concentrations of about 1% paclitaxel to polymer ratio found in the matrix after short-term release in 100% IPA.<sup>15</sup> In this study, the depth profile was close to zero, where 78% of the total drug (as measured by HPLC) was released. This indicates that the paclitaxel concentration in the SIBS film fell below 1% limit at that point. One of the ultimate objectives of this CARS study was to visualize paclitaxel distribution in DES. CARS microscopy has both forward and epi (reflected) signals. The epi-detected CARS will be highly useful for imaging a very thin polymer film coated on metal surfaces, such as on a stent. This project is under progress.

## References

- Edelman ER, Rogers C. Pathobiologic responses to stenting. *Am J Cardiol* 1998;81:4E-6E.
- Torres K, Horwitz SB. Mechanisms of Taxol-induced cell death are concentration dependent. *Cancer Res* 1998;58:3620-3626.
- Hwang CW, Wu D, Edelman ER. Stent-based delivery is associated with marked spatial variations in drug distribution. *J Am Coll Cardiol* 2001;37(2):1A-2A.
- Finkelstein A, McClean D, Kar S, Takizawa K, Varghese K, Baek N, Park K, Fishbein MC, Makkar R, Litvack F, Eigler NL. Local drug delivery via a coronary stent with programmable release pharmacokinetics. *Circulation* 2003;107:777-784.
- Westedt U, Wittmar M, Hellwig M, Hanefeld P, Greiner A, Schaper AK, Kissel T. Paclitaxel releasing films consisting of poly(vinyl alcohol)-*graft*-poly(lactide-*co*-glycolide) and their potential as biodegradable stent coatings. *J Control Release* 2006;111:235-246.
- Acharya G, Park K. Mechanism of controlled drug release from drug-eluting stents. *Adv Drug Delivery Rev* 2006;58:387-401.
- van der Weerd J, Kazarian SG. Combined approach of FTIR imaging and conventional dissolution tests applied to drug release. *J Control Release* 2004;98:295-305.
- Bobiak JP, Koenig JL. Regions of interest in FTIR imaging applications: Diffusion of nicotine into ethylene-*co*-vinyl acetate films. *J Control Release* 2005;106:329-338.
- Coutts-Lendon C, Koenig JL. Investigation of the aqueous dissolution of semicrystalline poly(ethylene oxide) using infrared chemical imaging: The effects of molecular weight and crystallinity. *Appl Spectrosc* 2005;59:976-985.
- Feofanov AV, Grichine AI, Shitova LA, Karmakova TA, Yakubovskaya RI, Egret-Charlier M, Vigny P. Confocal Raman microspectroscopy and imaging study of theraphthal in living cancer cells. *Biophys J* 2000;78:499-512.
- Wartewig S, Neubert RHH. Pharmaceutical applications of mid-IR and Raman spectroscopy. *Adv Drug Delivery Rev* 2005;57:1144-1170.
- Ashraf M, Luorno VL, Coffinbeach D, Evans CA, Augsburg LL. A novel nuclear-magnetic-resonance (NMR) imaging method for measuring the water front penetration rate in hydrophilic polymer matrix capsule plugs and its role in drug-release. *Pharm Res* 1994;11:733-737.
- Verhoeven M, Driessen AAG, Paul AJ, Brown A, Canry JC, Hendriks M. DSIMS characterization of a drug-containing polymer-coated cardiovascular stent. *J Control Release* 2004;96:113-121.
- Belu AM, Davies MC, Newton JM, Patel N. TOF-SIMS characterization and imaging of controlled-release drug delivery systems. *Anal Chem* 2000;72:5625-5638.
- Kang E, Wang H, Kwon IK, Robinson J, Park K, Cheng J-X. In situ visualization of paclitaxel distribution and release by coherent anti-Stokes Raman scattering microscopy. *Anal Chem* 2006;78:8036-8043.
- Cheng JX, Xie XS. Coherent anti-Stokes Raman scattering microscopy: Instrumentation, theory, and applications. *J Phys Chem B* 2004;108:827-840.
- Cheng JX. Coherent anti-Stokes Raman scattering microscopy. *Appl Spectrosc* 2007;61:197A-208A.
- Ranade SV, Miller KM, Richard RE, Chan AK, Allen MJ, Helmus MN. Physical characterization of controlled release of paclitaxel from the TAXUS<sup>TM</sup> Express<sup>2TM</sup> drug-eluting stent. *J Biomed Mater Res A* 2004;71:625-634.
- Ranade SV, Richard RE, Helmus MN. Styrenic block copolymers for biomaterial and drug delivery applications. *Acta Biomater* 2005;1:134-144.
- Kamath KR, Barry JJ, Miller KM. The Taxus drug-eluting stent: A new paradigm in controlled drug delivery. *Adv Drug Delivery Rev* 2006;58:412-436.
- Cheng JX, Jia KY, Zheng G, Xie XS. Laser-scanning coherent anti-Stokes Raman scattering microscopy and applications to cell biology. *Biophys J* 2002;83:502-509.
- Li L, Wang H, Cheng JX. Quantitative coherent anti-Stokes Raman scattering imaging of lipid distribution in co-existing domains. *Biophys J* 2005;89:3480-3490.
- Coutts-Lendon CA, Wright NA, Mieso EV, Koenig JL. The use of FT-IR imaging as an analytical tool for the characterization of drug delivery systems. *J Control Release* 2003;93:223-248.
- Siepmann J, Streubel A, Peppas NA. Understanding and predicting drug delivery from hydrophilic matrix tablets using the "sequential layer" model. *Pharm Res* 2002;19:306-314.
- Siepmann J, Peppas NA. Modeling of drug release from delivery systems based on hydroxypropyl methylcellulose (HPMC). *Adv Drug Delivery Rev* 2001;48(2/3):139-157.
- Siepmann J, Faisant N, Benoit JP. A new mathematical model quantifying drug release from bioerodible microparticles using Monte Carlo simulations. *Pharm Res* 2002;19:1885-1893.